

## Postnatal development of thalamic reticular nucleus projections to the anterior thalamic nuclei in rats

Hitoshi Fujita, Kosuke Imura, Masahito Takiguchi, Kengo Funakoshi

Department of Neuroanatomy, Graduate School of Medicine, Yokohama City University, Yokohama, Japan

### ABSTRACT

The thalamic reticular nucleus (TRN) projects inhibitory signals to the thalamus, thereby controlling thalamo-cortical connections. Few studies have examined the development of TRN projections to the anterior thalamic nuclei with regard to axon course and the axon terminal distributions. In the present study, we used parvalbumin (PV) immunostaining to investigate inhibitory projections from the TRN to the thalamus in postnatal (P) 2- to 5-week-old rats (P14–35). The distribution of PV-positive (+) nerve fibers and nerve terminals markedly differed among the anterior thalamic nuclei at P14. Small, beaded nerve terminals were more distributed throughout the anterodorsal nucleus (AD) than in the anteroventral nucleus (AV) and anteromedial nucleus (AM). PV+ fibers traveling from the TRN to the AD were observed in the AV and AM. Nodular nerve terminals, spindle or *en passant* terminals, were identified on the axons passing through the AV and AM. At P21, axon bundles traveling without nodular terminals were observed, and nerve terminals were distributed throughout the AV and AM similar to the AD. At P28 and P35, the nerve terminals were evenly distributed throughout each nucleus. In addition, DiI tracer injections into the retrosplenial cortex revealed retrogradely-labeled projection neurons in the 3 nuclei at P14. At P14, the AD received abundant projections from the TRN and then projected to the retrosplenial cortex. The AV and AM seem to receive projections with distinct nodular nerve terminals from the TRN and project to the retrosplenial cortex. The projections from TRN to the AV and AM with nodular nerve terminals at P14 are probably developmental-period specific. In comparison, the TRN projections to the AD at P14 might be related to the development of spatial navigation as part of the head orientation system.

**Key words:** Thalamic reticular nucleus; parvalbumin; axon terminal; development; anterior thalamic nucleus; rat.

**Correspondence:** Kosuke Imura, Department of Neuroanatomy, Graduate School of Medicine, Yokohama City University, 3-9 Fukuura, Kanazawa-ku, Yokohama, 236-0004, Japan. Tel. +81.045.7872571.  
E-mail: imurako@yokohama-cu.ac.jp

**Contributions:** HF, performed the experiments; KI, MT, supervised the experimental procedures; KI, designed the study; HF, KI, analyzed and discussed the data; HF, KI, writing the manuscript; KI, KF, supervised the study. The authors have read and approved the final version of manuscript.

**Conflict of interest:** The authors declare no conflict of interest.

**Ethics approval:** This study is approved under the guidelines of the official Japanese regulations for research on animals in the Yokohama City University (approval NO. F-A-16-064).

**Funding:** Supported by the Fundamental Research Funding of Yokohama City University.

## Introduction

The thalamus relays primarily sensory information locally to the cortex (thalamocortical tract) and receives descending projections from the cortex (corticothalamic tract). These reciprocal contacts with the cerebral cortex are closely related to sensory, motor, and higher brain functions. The neurons that make up the thalamus include excitatory neurons that project to the cerebral cortex and interneurons that inhibit the projection neurons.<sup>1</sup> In addition to interneurons, neurons in the thalamic reticular nucleus (TRN) exert extrinsic inhibitory control over projection neurons. The TRN covers the lateral side of the thalamus in the frontal section and is continuous from the anterior to posterior thalamic nuclei. The TRN projections do not project to the cerebral cortex, but send inhibitory gamma-aminobutyric acid (GABA) signals to the thalamus.<sup>2</sup> The TRN also receives input from axonal collateral branches originating in the thalamocortical and corticothalamic tracts,<sup>2</sup> and some of the neurons project to the contralateral TRN, indirectly sending information to the contralateral thalamus as well.<sup>3</sup> Therefore, the TRN is considered to be an important nucleus and gate guardian that coordinates communication between the thalamus and cerebral cortex.<sup>2</sup>

In mammals, communication between the thalamus and cerebral cortex, including the TRN, is homologous among species, but the distribution and number of projection neurons and interneurons in the thalamus vary. In cats and monkeys, approximately 70% of all neurons in most nuclei are projection neurons, and the remaining 30% are interneurons.<sup>4,5</sup> In the rat thalamus, however, interneurons are absent in many nuclei.<sup>4,5</sup> Therefore, the TRN is reported to be the largest exogenous source of inhibitory control of thalamocortical communication in rats.<sup>2</sup>

Although major inhibitory projections from the TRN play an essential role in thalamocortical communication, few studies have examined the developmental stages of the TRN compared with research on the developmental stages of inhibitory neurons in the neocortex.<sup>6</sup> In rats, most neurons in the TRN are calcium-binding protein, parvalbumin-positive (PV+) neurons that coexpress GABA, while other thalamic projection neurons do not express PV.<sup>7,8</sup> The expression of PV as a marker for the TRN has been observed by immunostaining, and changes during postnatal development have been reported.<sup>9-11</sup> In these reports, the distributions of PV+ nerve fibers and nerve terminals, which are thought to originate from the TRN, are observed as a gradient pattern from the lateral to the medial thalamus during development.<sup>9,11</sup> By approximately 30 days after birth, the distribution of PV+ terminals from the TRN is similar to that of adults.<sup>9</sup> Differences in the distribution of nerve fibers in each thalamic nucleus and the detailed structure of the nerve terminals, however, have not been clarified. In particular, very few studies have investigated the development of the TRN projections to the anterior thalamic nuclei (anterodorsal nucleus: AD, anteroventral nucleus: AV, and anteromedial nucleus: AM) with regard to axon course and axon terminal distributions.<sup>10,11</sup> The anterior thalamic nuclei play essential roles in spatial cognitive functions and memory, and are involved in exploratory behavior in rats.<sup>12,13</sup> These functions are served by the limbic system, in which the anterior thalamic nuclei communicate with the cerebral cortex, hippocampal formation, and subcortical structures such as mammillary body.<sup>14</sup>

In the present study, we investigated the development of projections from the TRN at the axonal level to observe in detail the inhibitory projections of TRN efferents that regulate communication between the thalamus and cerebral cortex in normal rats. PV immunostaining was performed in the thalamus at two weeks of age (P14), three weeks of age (P21), four weeks of age (P28), and five weeks of age (P35). Furthermore, projections from the anterior

or thalamic nuclei to the cerebral cortex were investigated by injecting the neural circuit with carbocyanine fluorescent dyes to label projection neurons in the thalamic nuclei at P14.

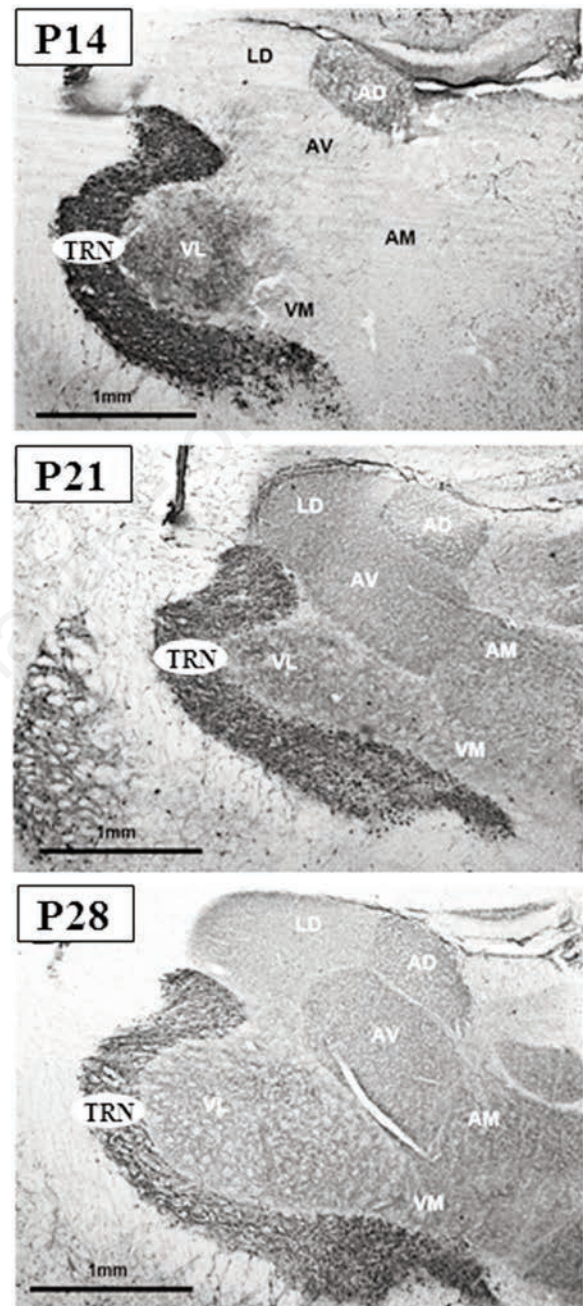


**Figure 1.** Immunohistochemistry of parvalbumin (PV) in postnatal 2 to 4 weeks-old rats (P14–28). Note PV-positive nerve fibers and nerve terminals was markedly altered among the anterior thalamic nuclei. In P14, differences in the distribution of PV+ fibers and nerve terminals are shown. In the AD, small beaded nerve terminals are more distributed throughout the nucleus than in the AV and AM. AD, anterodorsal nucleus; AM, anteromedial nucleus; AV, anteroventral nucleus; LD, laterodorsal nucleus; TRN, thalamic reticular nucleus; VL, ventral lateral nucleus; VM, ventral medial nucleus. Scale bar : 1mm.

## Materials and Methods

### Animals

A total of 26 neonatal Wistar rats (SLC, Shizuoka, Japan) were used in this study. The original research reported herein was performed under the official Japanese regulations for animal research guidelines and approved by Yokohama City University (approval No. F-A-16-064). Postnatal rat pups were used for PV immunohistochemistry (P14, n=3; P21, n=4; P28, n=3; P35, n=6). Additionally, P14 (n=10) rat pups were used for the neural tract tracing experiments using carbocyanine fluorescent dyes, such as DiI.

### Fixation and tissue preparation

All animals were deeply anesthetized with isoflurane gas and perfused transcardially with 4% paraformaldehyde (PFA) in 0.1 M phosphate-buffered saline (PBS; pH 7.4). Brains were removed from skulls and postfixed with 4% PFA overnight at 4°C. For PV immunohistochemistry, after being cryoprotected by soaking overnight in 20% sucrose in PBS, the brains were embedded in OCT compound (Sakura Finetechnical Co., Tokyo, Japan) and frozen rapidly by immersing them in a cold isopentane liquid. The brain blocks were cut transversely at a thickness of 40 µm on a cryostat (CM3050S, Leica, Wetzlar, Germany). The serial sections were collected in PBS at 4°C. For the DiI injections, the postfixed brains were divided into 2 blocks transversely using small razor blades at the level of the anterior thalamus.

### PV immunohistochemistry

The sections were incubated with mouse monoclonal anti-PV antibody (1:10,000; Clone PARV-19, Sigma, Darmstadt, Germany) for 2 days at 4°C after immersing them in blocking solution (0.1 M PBS containing 0.01% Tween 20, and 5% normal goat serum) for 60 min at room temperature. The anti-PV antibody specificity was confirmed by western blot analysis.<sup>15</sup> The rat TRN was well labeled by immunohistochemistry with the antibody<sup>16</sup> but not in

the PV knockout mice.<sup>17</sup> After primary antibody incubation, endogenous peroxidase activity was blocked by soaking the sections in 0.01% H<sub>2</sub>O<sub>2</sub> in PBS for 10 min at room temperature. The sections were then incubated with biotinylated anti-mouse secondary goat antibody (1:200; Vector Laboratories, Burlingame, CA, USA) for 60 min at room temperature and visualized using avidin-biotin complex-conjugated horseradish peroxidase (ABC Elite kits; Vector Laboratories) with diaminobenzidine containing 0.03% nickel ammonium sulfate. Finally, the sections were mounted on gelatin-coated glass slides and coverslipped with Entellan® new (Merk, Darmstadt, Germany). Routine control for immunostaining was conducted during these experiments by omitting the anti-PV primary antibody.

### DiI tract tracing experiments

Injection of fluorescent carbocyanine dye (DiI; Molecular Probes, Eugene, OR) into the retrosplenial cortex (RSC) was performed in P14 fixed brain blocks. A DiI crystal was injected into the RSC of a divided brain using a fine insect pin under stereomicroscope. The brain was sealed with 5% gelatin and incubated in the 4% PFA at 37°C for 60 days. The tissue block was embedded in 5% gelatin and then sectioned transversely at 80 µm thickness using a micro slicer (3,000 W; DSK, Kyoto, Japan) or cut into 40 µm thick cryosections as described above.<sup>18</sup> The serial sections were observed under a fluorescence microscope equipped with a Texas red filter (DM-RE; Leica Microsystems, Wetzlar, Germany).

### Data analysis

All micrographs were taken as digital images (DM-RE; Leica Microsystems). PV+ immunoreactive fibers and terminals size in P14 anterior thalamic nuclei were assessed by generating the digital images. Pixels of the PV immunoreactive fibers and terminal sizes were measured as square microns in 2 nuclei (AD and AV) of 11 sections using ImageJ (<http://fiji.sc/Downloads>).<sup>19</sup> The ratio of the PV+ area was calculated for the whole area of each nucleus. The calculated ratio between two nuclei was compared statistically with a two-tailed *t*-test ( $p < 0.05$ ).

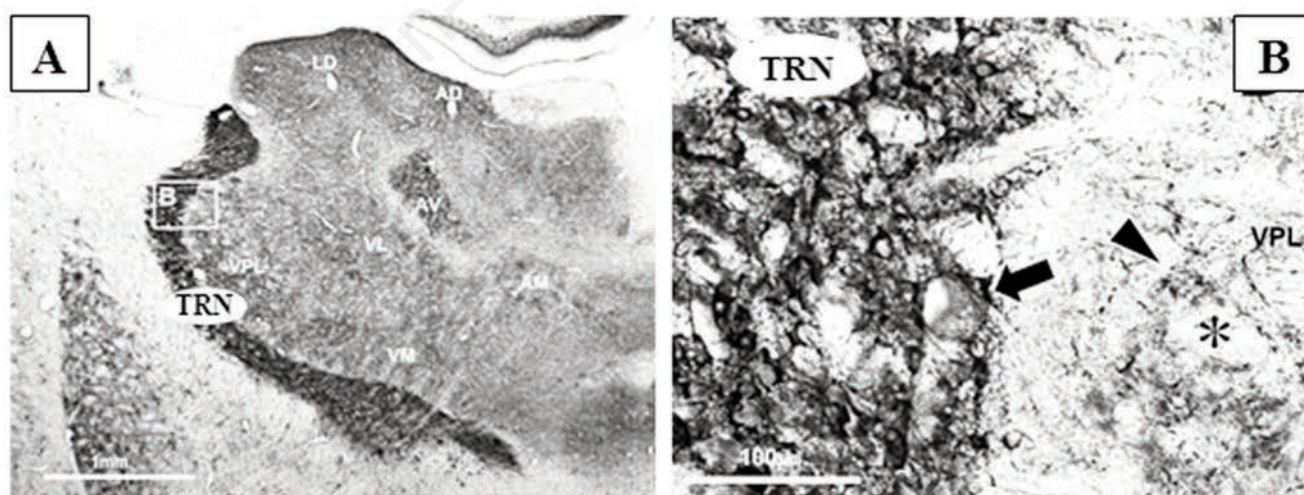


**Figure 2.** Immunohistochemistry of parvalbumin (PV) in postnatal 5 weeks-old rats (P35). A) PV-positive (+) terminals are entirely covered in all thalamic nuclei. A boxed region is re-photographed at higher magnification in B. B) An arrow indicate PV+ thalamic reticular nucleus. Small PV+ terminals are shown in ventral posterolateral nucleus (arrowhead). An asterisk indicates presumable cell body. AD, anterodorsal nucleus; AM, anteromedial nucleus; AV, anteroventral nucleus; LD, laterodorsal nucleus; TRN, thalamic reticular nucleus; VL, ventral lateral nucleus; VM, ventral medial nucleus; VPL, ventral posterolateral nucleus. Scale bars: A) 1 mm; B) 100 µm.

## Nomenclature

The 3 subdivisions of the anterior thalamic nuclei (AD, AV, and AM) were adopted based on an atlas<sup>20</sup> and delineated by observing Nissl-stained sections.

## Results

### PV immunohistochemistry in developing thalamus

We observed PV immunohistochemistry sections in the postnatal developing thalamus every week from P14 to P35 (Figures 1 and 2). At P14, neurons of the TRN were strongly PV-immunoreactive in the rostrocaudal regions (Figures 1 and 3). The PV+ fibers and terminals were observed in the ventral nuclei: the ventral posterolateral nucleus (VPL), ventral posteromedial nucleus, ventral lateral nucleus, ventral medial nucleus, laterodorsal nucleus, lateral geniculate nucleus, and lateral posterior nucleus (Figures 1 and 3). In contrast to the PV+ thalamic nuclei, the anterior thalamic nuclei exhibited different staining patterns (Figure 3). Sparse PV+ fibers and terminals were scattered in the AV and AM (Figures 3 to 5). The PV+ fibers passed mainly through the AV lateromedially, but very dense, small, beaded PV+ terminals were observed throughout the AD (Figures 4 and 5). After P21, the PV+ terminals appeared denser in the AV and AM (Figures 1 and 2). Finally, by P35, the PV+ terminals entirely covered all the thalamic nuclei (Figure 2).

### PV+ fibers and terminals in the anterior thalamus at P14

We traced the trajectory of the PV+ fibers in the AV and AM. The PV+ fibers came from the TRN and ran mainly through the AV (Figures 4A and 5A). Fibers with nodular, spindle, or *en passant* terminals were heading lateromedially into the AD (Figures 4 C-D and 5 C-D). Many small PV+ terminals with fine fibers were then distributed in the AD (Figures 4B and 5A). These terminals were observed as perisomatic patterns and seemed to terminate the AD neurons (Figure 4B). At P14, the PV+ fibers and terminals in the 2 nuclei exhibited clearly different patterns, sparse running fibers in the AV or dense distributing terminals in the AD (Figure 5 A,B). We measured the ratio of the PV+ fibers and terminals as pixels for the whole area of each of the 2 nuclei. The median PV+ staining density in the AD and AV was 0.35 and 0.07, respectively (Figure 6). The distribution of PV+ fibers and terminals was significantly denser in the AD than in the AV (Figure 6,  $*p < 0.05$ ).

### DiI labeled neurons in the anterior thalamus at P14

We injected DiI crystals into the ipsilateral RSC to confirm the thalamocortical projections from the AV, AD, and AM at P14 (Figure 7). The injected DiI diffusion was restricted in the RSC (Figure 7A). Some retrogradely labeled neurons were observed in the anterior thalamus after the injections (Figure 7 B,C). In the AV and AD, the labeled neurons were scattered throughout the whole region (Figures 7 B-E), while sparsely labeled neurons were observed in the AM (Figure 7F). Some of the labeled fibers were distributed in these nuclei. We could not, however, distinguish the corticothalamic projections from these labeled fibers. An obvious DiI-labeled terminal morphology was not detected among our samples.

## Discussion

The developmental distribution patterns of PV immunoreactiv-

ity among the thalamus mostly corresponded with previous reports from P14 to P35.<sup>9-11</sup> Therefore, our PV immunohistochemistry was consistent with the postnatal development of the rat thalamus.

PV immunostaining revealed a marked change in the TRN projections to the anterior thalamic nuclei from P14 to P21. At P14,

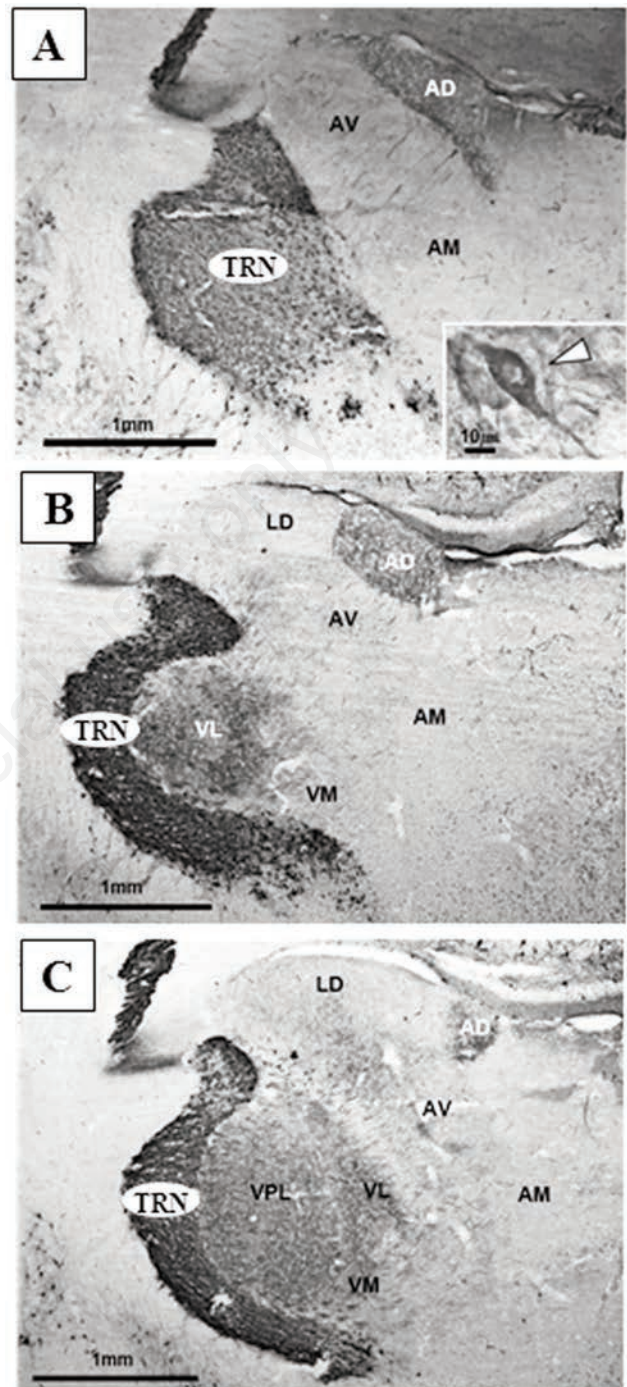


**Figure 3.** Immunohistochemistry of parvalbumin (PV) in rostro-caudal anterior thalamic nuclei in P14. Note rostro-caudal region in the AD (A to C), PV+ small beaded nerve terminals are more distributed throughout the nucleus than in the AV and AM. A PV+ neuron in TRN at higher magnification is shown in A (arrowhead in right inset). AD, anterodorsal nucleus; AM, anteromedial nucleus; AV, anteroventral nucleus; LD, laterodorsal nucleus; TRN, thalamic reticular nucleus; VL, ventral lateral nucleus; VM, ventral medial nucleus; VPL, ventral posterolateral nucleus. Scale bars: A-C) 1 mm; inset in A) 10 µm.

the AD already received abundant projections with small perisomatic terminations from the TRN, and although the AV and AM had fewer such projections than the AD when observed at the single axon level, distinct nodular nerve terminals, spindle or *en passant* terminals, were observed on axons passing through the AV and AM. By P21, a few nodular terminals were observed, and the AV and AM received as many projections from the TRN as the AD received. This suggests that the projections from the TRN with the nodular nerve terminals to the AV and AM at P14 were postnatal developmental stage-specific.

Previous studies reported that the PV+ nerve terminals are distributed throughout the AV of P22 rats.<sup>9</sup> Seto-Ohshima *et al.*<sup>10</sup> observed PV+ fiber segments running through AV, and PV+ small terminals in the AD in P11 rats. The present results are consistent with these reports, although the developmental stage at P14 in our samples was later than Seto-Ohshima *et al.*<sup>10</sup> The previous studies, however, reported no developmentally specific PV+ nodular nerve terminals in the AV and AM. In guinea pigs at P20, PV immuno-

staining of the anterior thalamic nuclei showed more abundant PV+ nerve terminals in the AD than in the AV and AM.<sup>21</sup> These findings indicate a typical distribution pattern of PV in rodent anterior thalamic nuclei.<sup>22</sup> The morphology of time-specific nodular nerve terminals in P14 are similar to TRN-derived GABA-positive nerve terminals distributed in the ventral basal nuclei of rats observed by 3 weeks of age.<sup>23</sup> Electron microscopic observations of these nerve terminals indicated that the synaptic structures matured by the end of the first 2 weeks of life.<sup>23</sup> In addition, PV+ *en passant* terminals on dendrites were observed in rat VPL at P7 by electron microscopy.<sup>11</sup> It is unclear whether the nodular and *en passant* terminals observed in this study are matured GABAergic synapses on projection neurons in the AV or AM. At P14, however, DiI-labeled neurons of the anterior thalamic nuclei project to the RSC so these nerve terminals may be in functional contact with thalamic projection neurons. Axons with nodular nerve terminals reached the AD border, but whether they project to the AD at the same time as to the AV or AM was not confirmed. We observed

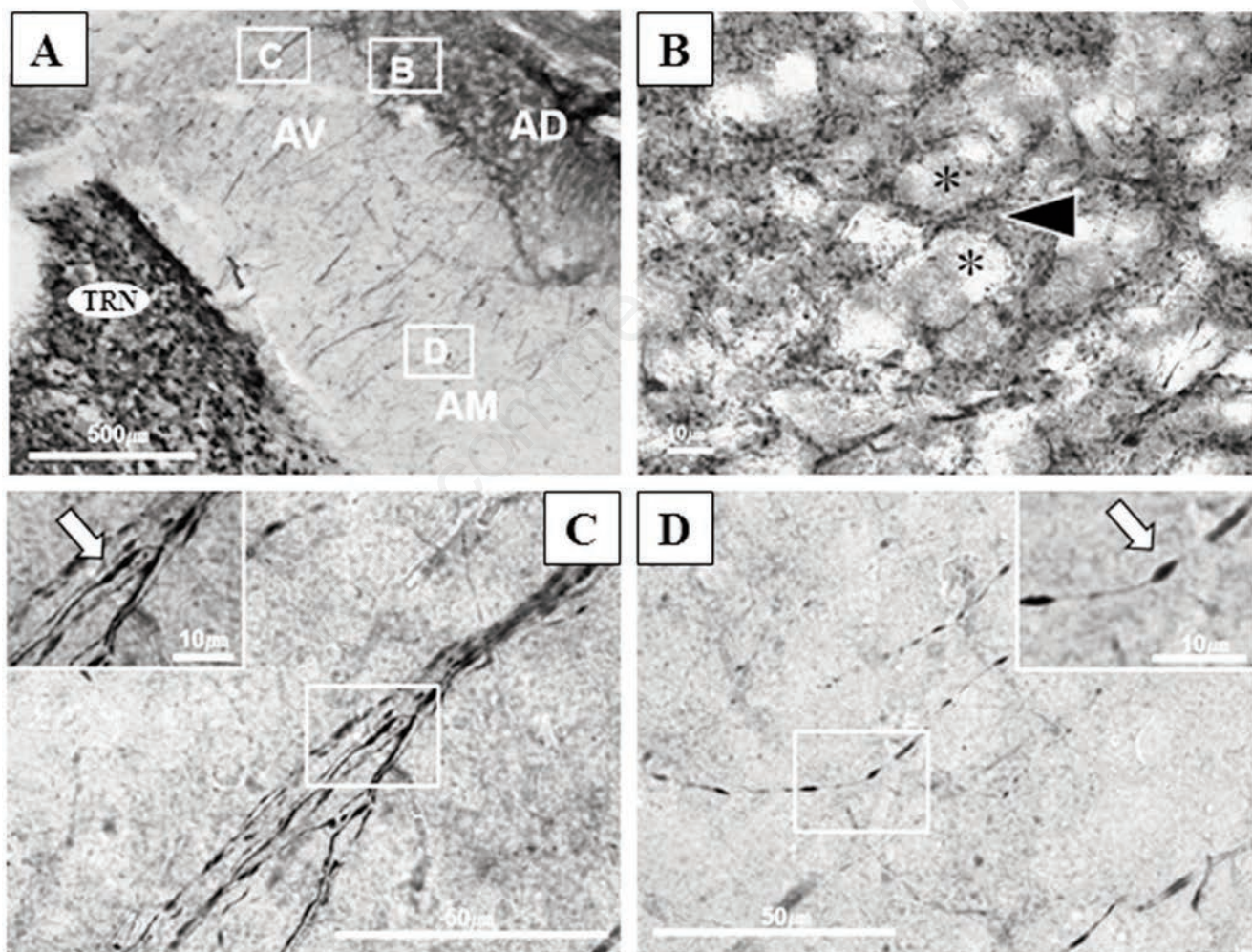


**Figure 4.** PV+ fibers and terminals in anterior thalamic nuclei (P14). A) Low magnification of the anterior thalamic nuclei and TRN. Three boxed regions are re-photographed at higher magnification in B-D. B) Dense PV+ small beaded nerve terminals are shown as perisomatic patterns (arrow head) in AD. Asterisks indicate presumable cell bodies. C,D) PV+ fibers with nodular, spindle, or *en passant* terminals, running through AV and dorsal border region between AV and AM. Boxed regions are represented at higher magnification in left and right insets. Arrows indicate terminals. AD, anterodorsal nucleus; AM, anteromedial nucleus; AV, anteroventral nucleus; TRN, thalamic reticular nucleus. Scale bars: A) 500  $\mu\text{m}$ ; B) 10  $\mu\text{m}$ ; C and D insets) 10  $\mu\text{m}$ ; C,D) 50  $\mu\text{m}$ .

that a small number of terminals terminated in the AD from the axons that reached them, but further tracing of the axons that reached the AD was difficult due to the barrier of PV<sup>+</sup> terminals that were densely distributed in the AD (Figure 5 B,C).

We confirmed the projections from the 3 anterior thalamic nuclei to the RSC at P14 using DiI retrograde labeling. Previously, cortical projections from zinc-positive AD neurons were confirmed during the second postnatal week, from P9 to P13, by cortical injections of sodium selenite.<sup>24</sup> This cortical projection was only labeled with specific zinc-positive AD neurons, but AV and AM neurons were not detected as zinc-positive projections.<sup>24</sup> Our observation of the PV<sup>+</sup> small perisomatic terminations in the AD seems to overlap with the zinc-positive neurons in the postnatal developmental stage. Therefore, the TRN projection to the AD might be related to specific zinc-positive thalamocortical projections during postnatal development. Further studies are needed, however, to determine if TRN projections terminate on zinc-positive AD projection neurons during the second postnatal week.

The AD contributes to spatial navigation as part of the head orientation system, including so-called head direction (HD) cells.<sup>12,13</sup> It is assumed that the HD cells receive TRN projections in the AD thalamocortical projection. Therefore, it is essential to discuss the development of projections from the TRN to the AD. Furthermore, the HD circuitry in the AD is reported to be somewhat complete before the animal's eyes open,<sup>13,25</sup> and its function becomes more stable as soon as the eyes open at around P12-16.<sup>25</sup> Thus, the reason that the projections from the TRN to the AD and the AD projections to the cortex are already established by P14 is probably that the HD system immediately utilizes the visual information carried by these projections.<sup>13,25</sup> As some visual input to the AD comes from other cortical areas<sup>20,21</sup> and some come directly from the retina,<sup>26</sup> these projections may be completed early on to adequately process information from such pathways. In addition to this input to the AD, it is known to receive projections from the mammillary body.<sup>27</sup> It is also important for the head orientation system to work that vestibular input is carried by the mammi-

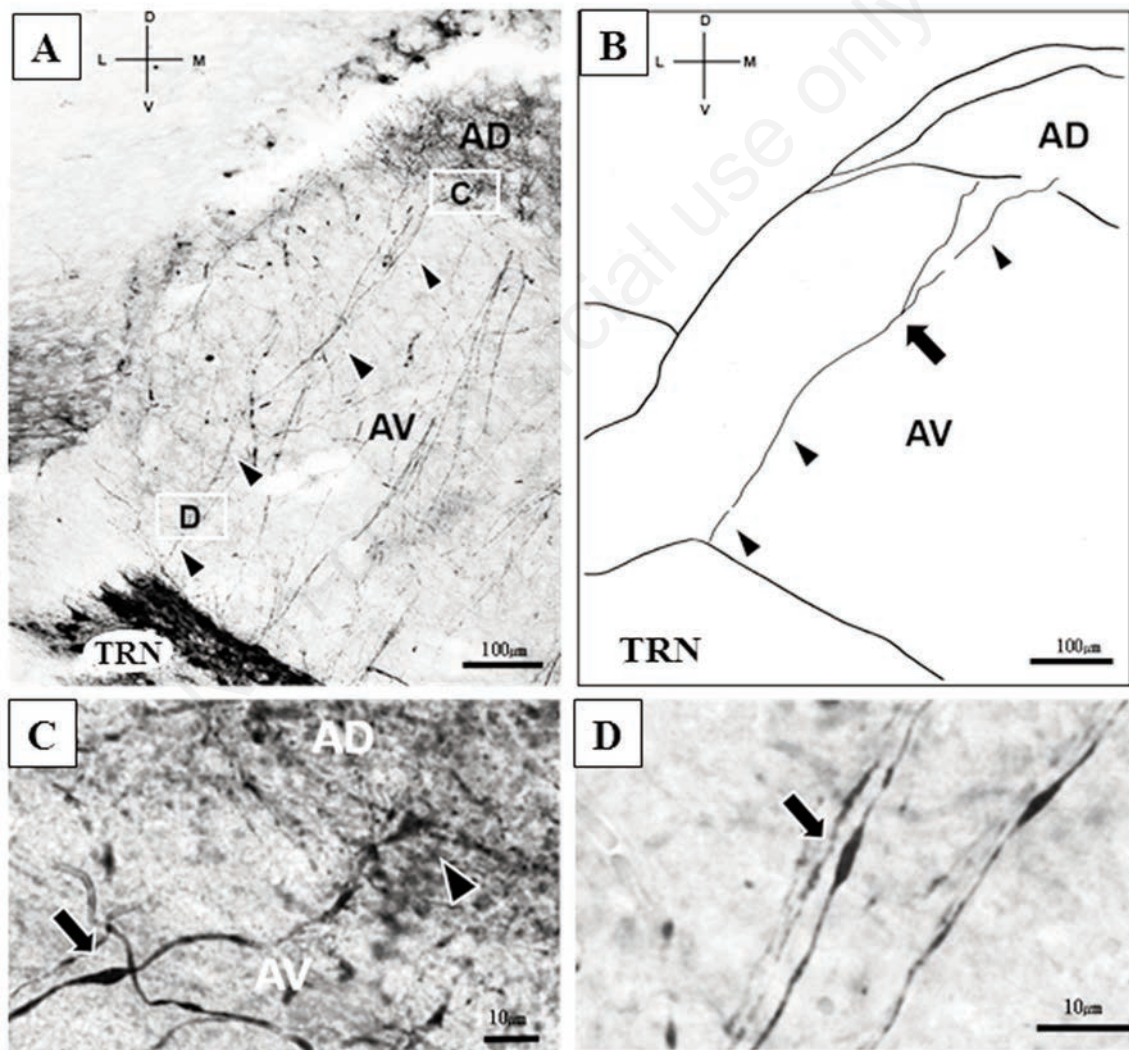


**Figure 5.** Trajectory of the PV<sup>+</sup> fiber in AV (P14). A) Low magnification of the AV. Arrowheads indicate a single PV<sup>+</sup> fiber which is traced in B; two boxed regions of the single PV<sup>+</sup> fiber are re-photographed at higher magnification in C and D. B) Depicted line drawing of the single PV<sup>+</sup> fiber in A is running through AV (arrowheads); an arrow indicates a branch; note the fiber is running from TRN to AD. C) The PV<sup>+</sup> fiber with terminals (arrow); arrowhead indicate a terminal at edge of AD. D) An arrow indicates terminal in AV. AD, anterodorsal nucleus; AM, anteromedial nucleus; AV, anteroventral nucleus; TRN, thalamic reticular nucleus. Scale bars: A,B) 100 μm; C,D) 10 μm.

thalamic projection through the tegmental dorsal nucleus.<sup>28</sup> Postnatal projection from the mammillary body is established with the medial nucleus projecting ipsilaterally to AV and AM, and the lateral nucleus projecting bilaterally to AD from P8.<sup>29</sup> Celio<sup>7</sup> reported that PV-positive neurons were mainly found in the medial nucleus and to a lesser extent in the lateral nucleus. Frassoni *et al.*<sup>9</sup> depicted PV+ fiber bundle in the mammillo-thalamic tract at P22 in their figure 4. However, we could not observe PV+ fibers in the mammillo-thalamic tract at P14. The mammillo-thalamic projections other than PV+ nerve fibers may be responsible for this neural circuit at P14.

## Acknowledgments

We thank the members of the Department of Neuroanatomy at Yokohama City University for their advice and cooperation.

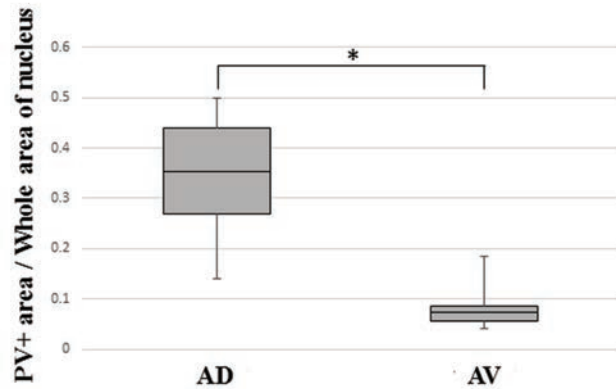


**Figure 6.** Ratio of PV+ fibers and terminals as pixels in the whole area of AD and AV. The median of the PV+ in AD and AV are 0.35 and 0.07 respectively. The AD was significantly denser than the PV+ fibers and terminals in the AV (\* $p < 0.05$ ).

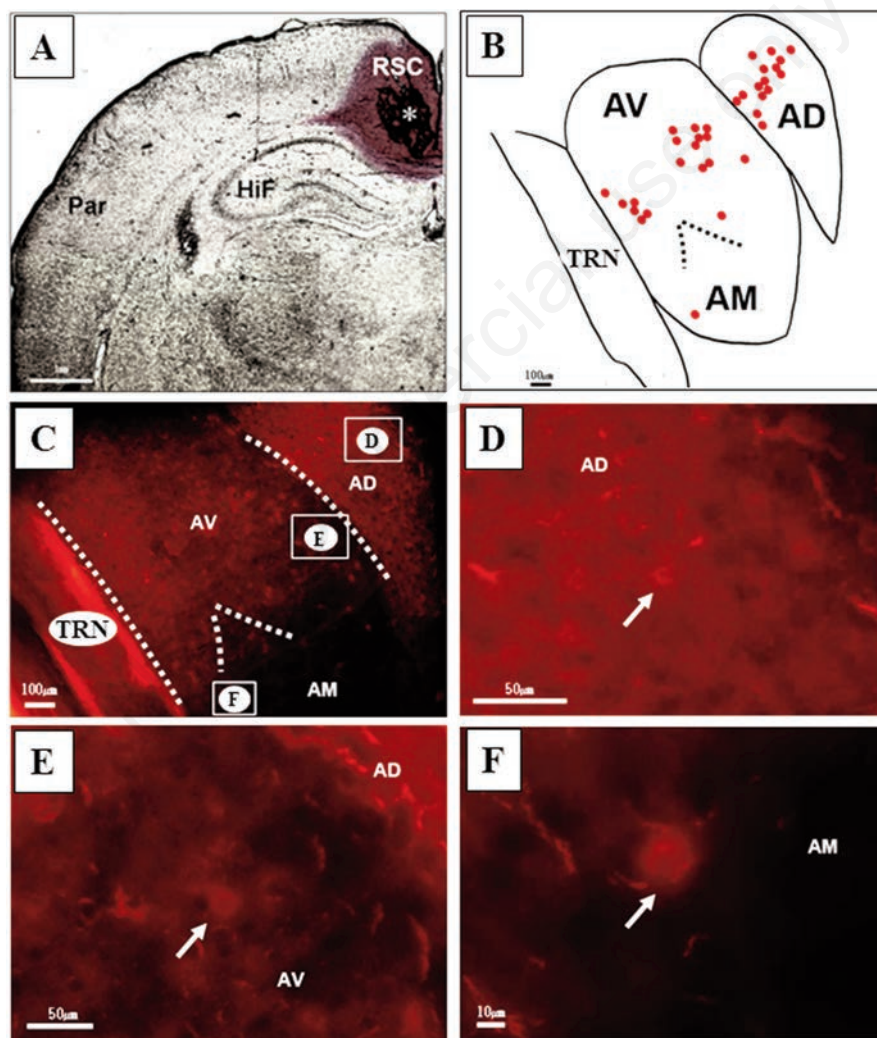


**Figure 7.** Retrogradely labeled neurons in anterior thalamic nuclei after an injection of DiI to retrosplenial cortex (P14). A) Low magnification of the injection site (asterisk). B) Line drawing of distributions of labeled projection neurons in anterior thalamic nuclei; red circles indicate labeled neurons; C) Low magnification of anterior thalamic nuclei after the DiI injection; three boxed regions are re-photographed at higher magnification in D-F. D) Retrogradely labeled neurons in AD (arrow). E) Retrogradely labeled neurons in AV (arrow). F) A retrogradely labeled neuron in AM (arrow). AD, anterodorsal nucleus; AM, anteromedial nucleus; AV, anteroventral nucleus; HiF hippocampal formation; RSC, retrosplenial cortex; Par, parietal cortex; TRN, thalamic reticular nucleus. Scale bars: A) 1 mm; B,C) 100  $\mu\text{m}$ ; D,E) 50  $\mu\text{m}$ ; F) 10  $\mu\text{m}$ .

## References

1. Jones EG. Thalamic circuitry and thalamocortical synchrony. *Phil Trans R Soc Lond B* 2002;357:1659-73.
2. Takata N. Thalamic reticular nucleus in the thalamocortical loop. *Neurosci Res* 2020;156:32-40.
3. Battaglia G, Lizier C, Colacitti C, Princivale A, Spreafico R. A reticuloreticular commissural pathway in the rat thalamus. *J Comp Neurol* 1994;347:127-38.
4. Arcelli P, Frassoni C, Regondi CM, De Biasi S, Spreafico R. GABAergic neurons in mammalian thalamus: a marker of thalamic complexity? *Brain Res Bull* 1997;42:27-37.
5. Sherman SM. Interneurons and triadic circuitry of the thalamus. *Trends Neurosci* 2004;27:670-5.
6. Murata Y, Colonnese MT. Thalamic inhibitory circuits and network activity development. *Brain Res* 2019; 706:13-23.
7. Celio MR. Calbindin D-28k and parvalbumin in the rat nervous system. *Neuroscience* 1990;135:375-475.
8. Arai R, Jacobowitz DM, Deura S. Distribution of calretinin, calbindin-D28k, and parvalbumin in the rat thalamus. *Brain Res Bull* 1994;33:595-614.
9. Frassoni C, Bentivoglio M, Spreafico R, Sánchez MP, Puelles L, Fairen A. Postnatal development of calbindin and parvalbumin immunoreactivity in the thalamus of the rat. *Develop Brain Res* 1991;58:243-9.
10. Seto-oshima A, Aoki E, Semba R, Emson PC, Heizmann CW. Parvalbumin immunoreactivity in the reticular thalamic nucleus of developing rats. *Acta Histochem Cytochem* 1989;22:331-40.
11. Amadeo A, Ortino B, Frassoni C. Parvalbumin and GABA in the developing somatosensory thalamus of the rat: an immunocytochemical ultrastructural correlation. *Anat Embryol (Berl)* 2001;203:109-19.
12. Yoder RM, Clark BJ, Taube JS. Origins of landmark encoding in the brain. *Trends Neurosci* 2011;34:561-71.
13. Tan HM, Bassett JP, O'Keefe J, Cacucci F, Wills TJ. The development of the head direction system before eye opening in the rat. *Curr Biol* 2015;25:479-83.
14. Perry BAL, Mitchell AS. Considering the evidence for anterior and laterodorsal thalamic nuclei as higher order relays to cortex. *Front Mol Neurosci* 2019;12:167.
15. Liu XB, Coble J, van Luijtelaar G, Jones EG. Reticular nucleus-specific changes in alpha3 subunit protein at GABA synapses in genetically epilepsy-prone rats. *Proc Natl Acad Sci USA* 2007;104:12512-7.
16. Oda S, Funato H, Sato F, Adachi-Akahane S, Ito M, Takase K, Kuroda M. A subset of thalamocortical projections to the retrosplenial cortex possesses two vesicular glutamate transporter isoforms, VGluT1 and VGluT2, in axon terminals and somata. *J Comp Neurol* 2014;522:2089-106.
17. Burette AC, Strehler EE, Weinberg RJ. "Fast" plasma membrane calcium pump PMCA2a concentrates in GABAergic terminals in the adult rat brain. *J Comp Neurol* 2009 512:500-13.
18. Bartheld CSV, Cunningham DE, Rubel EW. Neuronal tracing with DiI: decalcification, cryosectioning, and photoconversion for light and electron microscopic analysis. *J Histochem Cytochem* 1990;38:725-33.
19. Schindelin J, Arganda-Carreras I, Frise E, Kaynig V, Longair M, Pietzsch T, et al. Fiji: an open-source platform for biological-image analysis. *Nat Methods* 2012;9:676-82.
20. Paxinos G, Watson C. The rat brain in stereotaxic coordinates. 2nd ed. Academic Press; 1986.
21. Zakowski W, Bogus-Nowakowska K, Robak A. Embryonic and postnatal development of calcium-binding proteins immunoreactivity in the anterior thalamus of the guinea pig. *J Chem Neuroanat* 2013;53:25-32.
22. Zakowski W. Neurochemistry of the anterior thalamic nuclei. *Mol Neurobiol* 2017;54:5248-63.
23. Biasi SD, Amadeo A, Arcelli P, Frassoni C, Spreafico R. Postnatal development of GABA-immunoreactive terminals in the reticular and ventrobasal nuclei of the rat thalamus: a light and electron microscopic study. *Neuroscience* 1997;76:503-16.
24. Miró-Bernié N, Ichinohe N, Pérez-Clausell J, Rockland KS. Zinc-rich transient vertical modules in the rat retrosplenial cortex during postnatal development. *Neuroscience* 2006;138:523-35.
25. Bassett JP, Wills TJ, Cacucci F. Self-organized attractor dynamics in the developing head direction circuit. *Curr Biol* 2018;28:609-15.
26. Ahmed AK, Guison NG, Yamadori T. A retrograde fluorescent-labeling study of direct relationship between the limbic (anterodorsal and anteroventral thalamic nuclei) and the visual system in the albino rat. *Brain Res* 1996;729:119-23.
27. Shibata H. Topographic organization of subcortical projections to the anterior thalamic nuclei in the rat. *J Comp Neurol* 1992;322:117-27.
28. Bassett J, Tullman ML, Taube JS. Lesions of the tegmentomammillary circuit in the head direction system disrupt the head direction signal in the anterior thalamus. *J Neurosci* 2007;27:7564-77.
29. Alpeeva EV, Makarenko IG. Perinatal development of the mammillothalamic tract and innervation of the anterior thalamic nuclei. *Brain Res* 2009;1248:1-13.

Received for publication: 14 December 2021. Accepted for publication: 26 February 2022.

This work is licensed under a Creative Commons Attribution-NonCommercial 4.0 International License (CC BY-NC 4.0).

©Copyright: the Author(s), 2022

Licensee PAGEPress, Italy

*European Journal of Histochemistry* 2022; 66:3370

doi:10.4081/ejh.2022.3370